DESIGN AND BUILDING OF TRANSMITTER AND RECEIVER FOR WIRELESS RESISTIVITY METER

BY

OLUWASEUN ADEYEYE

PG/PSC2110512

DEPARTMENT OF PHYSICS

FACULTY OF PHYSICAL SCIENCE

UNIVERSITY OF BENIN

BENIN CITY, NIGERIA

DECEMBER 2024

DESIGN AND BUILDING OF TRANSMITTER AND RECEIVER FOR WIRELESS RESISTIVITY METER

BY

OLLUWASEUN ADEYEYE

PG/PSC2110512

A THESIS SUBMITTED TO THE SCHOOL OF POSTGRADUATE STUDIES AS PART OF REQUIREMENT FOR THE AWARD OF THE DEGREE OF MASTERS OF SCIENCE IN ELECTRONICS IN THE DEPARTMENT OF PHYSICS, UNIVERSITY OF BENIN, BENIN CIYY, NIGERIA.

DECEMBER 2024

CERTIFICATION

We hereby certify that this thesis is an original research work carried out independently by **OLUWASEUN ADEYEYE** under the supervision of Prof. S. O. Azi, in fulfillment of the requirements for the award of the Degree of Master of Science (M.Sc.) in Electronics, Department of Physics, University of Benin, Benin City-Nigeria.

……. **…….**

PROF. S. O. AZI **DATE**

Project Supervisor

…… **…….**

PROF. CHRIS AIGBOGUN **DATE**

HEAD OF DEPARTMENT

……. **……**

EXTERNAL EXAMINER **DATE**

DEDICATION

This thesis is dedicated to God Almighty, whose presence, power, and wisdom have been my constant guide and strength throughout this journey.

CERTIFICATION OF THESIS/DISSERTATION ON PLAGIARISM

We the undersigned attest and declare that the thesis of OLUWASEUN ADEYEYE, titled Design of Transmitter and Receiver for Wireless Resistivity Meter, successfully passed the anti-plagiarism test and does not violate any copyright regulations.

…… ……

PROF. S. O. AZI **PROF. CHRIS AIGBOGUN**

Supervisor. **HOD, Physics.**

ACKNOWLEDGEMENTS

First and foremost, I acknowledge God Almighty, the Omniscient, for His presence, power, and wisdom that guided me throughout this journey. His grace and faithfulness have been my constant source of strength and inspiration.

I extend my heartfelt gratitude to my supervisor, Prof. S.O Azi who has been like a father to me. His love, accommodation, and unwavering support have been invaluable. He was always there to answer my questions and provide guidance, making this work possible.

I also appreciate the lecturers of the Department of Physics for their dedication and support. Their teachings have imparted in me the knowledge and skills necessary to accomplish this work. Special thanks to Prof. Taiwo Fawehinmi, who has always had my back and encouraged me to pursue further studies, and Mr. Elekofehinti Tosin for his consistent support.

To my loving parents, Mr. and Mrs. Adeyeye, I owe everything. Their prayers, love, and financial support have been my bedrock. They have always been there for me, providing anything I needed and more. My

siblings, especially Moyinoluwa, my brother, deserve my appreciation for their love, understanding, and encouragement.

My beloved fiancée, whose unwavering support and love inspire me to be the best version of myself, deserves a special mention. Her belief in me has been a source of strength and motivation.

I am grateful to my flatmates, Deborah Ologbo, Austin Adaiza, Favour Owumi, Emmanuel Oniyide and the entire Owumi family, for their kindness and companionship. Special thanks to Mummy Owumi, who has been like a mother to me, providing care and support in countless ways.

Finally, I appreciate my Apostolic Faith Church family for their love, prayers, and encouragement. Their unwavering support and faith in my success have been a significant part of my journey.

To everyone who contributed to this accomplishment in one way or another, I say a heartfelt thank you.

Contents

LIST OF TABLES

LIST OF FIGURES

ABSTRACT

This research focuses on the design and implementation of a wireless resistivity meter using discrete components. The system addresses the limitations of traditional wired resistivity meters by integrating a wireless transmitter and receiver for efficient data acquisition and portability. The transmitter processes sinusoidal and square wave signals from a signal generator and wirelessly transmits the data to a receiver for analysis.

The wireless resistivity meter was evaluated through experimental tests to validate its accuracy, reliability, and operational range. Results demonstrate that the system effectively captures and transmits geophysical data with high precision, making it a significant advancement over conventional wired systems. Key features of the system include real-time data storage and export capabilities, compatibility with modern software tools like LabVIEW Signal Express, and robust performance across varying field conditions.

This work contributes to knowledge by introducing a low-cost, portable solution for geophysical resistivity measurements, advancing from hardware-centric approaches to software-based systems. Additionally, the research sets the stage for future developments in geophysical instrumentation, including the integration of IoT technologies, enhanced communication protocols, and energy-efficient designs.

The wireless resistivity meter offers a promising alternative for geophysical explorations, bridging the gap between traditional methods and modern technological advancements.

CHAPTER ONE

INTRODUCTION

1.1 BACKGROUND OF THE STUDY

The electrical resistivity method is a geophysical technique widely used for subsurface investigations. It involves the measurement of the resistance of the ground to the flow of electrical current. This method leverages the principle that different subsurface materials have distinct electrical resistivity values, which can be used to infer the presence of various geological structures, groundwater, and mineral deposits (Reynolds, 2011).

Electrical resistivity surveys are typically conducted by injecting current into the ground through a pair of electrodes and measuring the resulting potential difference at other electrodes. The apparent resistivity is then calculated using the geometric arrangement of the electrodes and the recorded measurements. Advances in instrumentation and data processing have made this method highly versatile for a range of applications, including environmental studies, engineering site investigations, and resource exploration (Telford et al., 1990).

The primary purpose of electrical resistivity surveys is to characterize subsurface properties without the need for extensive drilling or excavation. This non-invasive approach is particularly advantageous for assessing groundwater potential, detecting contamination, mapping bedrock, and identifying structural anomalies. For instance, groundwater exploration often relies on resistivity methods to locate aquifers, as water-bearing formations typically exhibit lower resistivity values compared to surrounding rocks (Kearey et al., 2002).

The development of wireless resistivity meters represents a significant technological advancement in this field. Traditional resistivity surveys require extensive cabling and manual setup, which can be labor-intensive and time-consuming. By integrating wireless technology, modern resistivity meters aim to enhance efficiency, reduce logistical challenges, and improve data acquisition in challenging terrains.

This study explores the design and implementation of a wireless resistivity meter. The goal is to develop a system that not only maintains the accuracy and reliability of conventional systems but also introduces flexibility and ease of deployment. By addressing the challenges of traditional methods, this project seeks to contribute to

the advancement of geophysical survey techniques and their practical applications in various fields.

In conclusion, the electrical resistivity method remains a cornerstone of geophysical exploration. Its continued evolution, particularly with the advent of wireless technologies, underscores its relevance in addressing modern scientific and engineering challenges. This study builds on this foundation, aiming to bridge the gap between traditional methods and emerging innovations in geophysical instrumentation.

1.2 RESISTIVITY INSTRUMENTATION

Resistivity instrumentation encompasses the tools and technologies used to measure electrical resistivity in subsurface investigations. A typical resistivity measurement system includes a current source, electrodes, and a voltmeter. The current source injects electrical current into the ground through current electrodes, while the potential electrodes measure the voltage difference caused by the current flow in the subsurface.

Modern resistivity meters are designed to be portable and efficient, featuring digital displays and advanced data storage capabilities. These devices often incorporate microprocessors to automate data collection and processing, making field operations more straightforward. Additionally, multi-electrode systems are commonly employed for larger surveys, enabling rapid data acquisition over extensive areas.

The introduction of wireless technology into resistivity instrumentation has further transformed the field. Wireless systems eliminate the need for cumbersome cabling, allowing for faster setup and greater flexibility in challenging environments. This innovation has paved the way for more efficient and accurate geophysical surveys, particularly in remote or inaccessible locations.

1.3 STATEMENT OF THE PROBLEM

Despite the widespread use of the electrical resistivity method, traditional resistivity instrumentation is often hindered by significant operational challenges. These include the cumbersome setup of electrode arrays using extensive cabling, which increases the time, labor, and costs associated with field surveys. In addition, harsh and

remote terrains pose logistical difficulties, limiting the accessibility and efficiency of conventional equipment.

Another critical issue is the lack of real-time data acquisition and processing capabilities in many existing systems. This shortfall can delay decision-making during field operations, particularly in time-sensitive investigations such as environmental assessments or disaster response efforts. Furthermore, the reliance on manual data handling introduces the risk of errors, compromising the accuracy and reliability of the survey results.

The advent of wireless technology offers an opportunity to overcome these limitations by introducing compact, flexible, and efficient systems for resistivity measurements. However, existing wireless resistivity meters are still in their infancy and often face challenges related to signal interference, data synchronization, and scalability for large-scale surveys. These issues underscore the need for further innovation and optimization in wireless resistivity instrumentation to meet the evolving demands of geophysical applications.

This study aims to address these gaps by designing and developing a wireless resistivity meter that integrates advanced data acquisition,

processing, and transmission features. By doing so, it seeks to enhance the efficiency, accuracy, and practicality of electrical resistivity surveys in diverse geological settings.

1.4 SIGNIFICANCE OF THE STUDY

The significance of this study lies in its potential to advance geophysical survey methodologies through the development of a wireless resistivity meter. This innovation addresses key challenges associated with traditional resistivity systems, such as cumbersome cabling, slow data acquisition, and operational inefficiencies. By introducing a compact and flexible solution, this study contributes to making resistivity surveys more accessible and practical for diverse applications.

One major area of impact is groundwater exploration, where the wireless resistivity meter can facilitate rapid and accurate identification of aquifers in both urban and remote settings. Additionally, environmental monitoring efforts, such as detecting soil contamination or tracking subsurface changes, will benefit from the improved efficiency and real-time capabilities of the proposed system.

In engineering and construction, the enhanced ease of deployment and scalability of wireless systems will support more effective site investigations, enabling timely decision-making for infrastructure development. Furthermore, this study has implications for academic research, as it provides a foundation for future innovations in resistivity instrumentation and fosters the integration of wireless technologies into geophysical practices.

Overall, this study bridges the gap between traditional resistivity methods and emerging technological trends, paving the way for more efficient, accurate, and user-friendly geophysical exploration tools.

1.5 SCOPE OF THE STUDY

This study focuses on the design, development, and evaluation of a wireless resistivity meter using the Wenner array configuration. The research emphasizes addressing the limitations of traditional resistivity systems by integrating wireless technology to enhance operational efficiency, data accuracy, and flexibility.

The scope includes the theoretical principles of electrical resistivity, the selection of suitable materials for instrumentation, and the development of a prototype system with wireless data acquisition and

transmission capabilities. Field testing will be conducted to validate the system's performance in diverse geological conditions, including urban and remote environments.

This study is limited to prototype development and validation, with future work anticipated for commercial scalability and broader applications. The emphasis remains on demonstrating the feasibility and benefits of the wireless approach for improving geophysical survey techniques.

1.6 AIM AND OBJECTIVES

The aim of this study is to design and build a wireless resistivity meter that overcomes the limitations of traditional wired systems.

The objectives are to;

1. design a wireless resistivity meter that eliminates the need for traditional cable-based systems.
2. Integrate real-time data transmission and remote control functionality to enhance usability.
3. Utilize cost-effective and readily available components to ensure affordability and accessibility.

4. Test the prototype in controlled environments to validate its performance against standard systems.
5. Develop a user-friendly interface to simplify data collection and analysis during field operations.
6. Optimize the design for diverse applications, including groundwater exploration and environmental studies.

CHAPTER TWO

LITERATURE REVIEW

2.1 THEORETICAL FOUNDATIONS OF ELECTRICAL RESISTIVITY

Electrical resistivity is a critical property that defines how materials oppose the flow of electrical current. It is mathematically expressed as:

$$R = \frac{\rho l}{A} \tag{2.1}$$

where ρ represents resistivity (measured in ohm-meters), R is the resistance (ohms), A is the cross-sectional area, and l is the length of the material through which current flows. The fundamental premise is that subsurface materials have varying resistivities, allowing geophysicists to map geological formations based on resistivity contrasts.

In resistivity surveys, electrodes are used to inject current into the ground while measuring the resulting potential differences. The Wenner array configuration is one of the simplest and most

widely used electrode arrangements. In this method, the electrodes are spaced at equal intervals, and the apparent resistivity is calculated using the formula:

$$\ell_a = \frac{\Delta V}{I} K \tag{2.2}$$

where ℓ_a is the apparent resistivity, K is the electrode spacing, ΔV is the measured potential difference, and I is the current injected. The Wenner array is particularly effective for shallow subsurface investigations due to its sensitivity and ease of deployment.

2.1.1 APPLICATIONS OF ELECTRICAL RESISTIVITY SURVEYS

Electrical resistivity surveys serve a diverse range of applications in geophysics, environmental science, engineering, and resource exploration. Some notable applications include:

1. **Groundwater Exploration**

   The detection and delineation of aquifers rely heavily on resistivity contrasts, as water-bearing formations typically

exhibit lower resistivity values compared to surrounding rocks. For example, Zohdy et al. (1974) demonstrated the effectiveness of resistivity surveys in identifying groundwater potential zones in arid regions.

2. **Environmental Studies**

   Resistivity methods are used to track contamination plumes, assess soil salinity, and map landfill boundaries. McNeill (1990) highlighted the utility of electrical resistivity in monitoring subsurface contamination due to industrial activities.

3. **Engineering Investigations**

   Geotechnical studies utilize resistivity surveys to determine bedrock depth, assess soil stability, and evaluate subsurface conditions for construction projects (Loke, 2000). These surveys provide critical data for the design and safety of infrastructure.

4. **Mineral Exploration**

   Ore bodies often exhibit distinct resistivity contrasts due to their metallic content. Keller & Frischknecht (1966) emphasized the role of resistivity methods in identifying and mapping economically viable mineral deposits.

2.2 Electrical Resistivity of Rocks and Minerals

Table 2.1: shows various values of resistivity of some common rocks, minerals and chemicals.

Materials	Resistivity (Ωm)	Conductivity (Siemen/m)
Igneous and Metamorphic Rock		
Granite	5× 103 – 106	10-6 - 2 x 10-4
Slate	6 x 102 – 4 x 107	2.5 x 10-8 1.7 x 10-3
Basalt	103 – 106	10-6 – 10-3
Marble	102 – 2.5 x 108	4 x 10-9 – 10-2
Quartzite	102 – 2 x 108	5 x 10-9 – 10-2
Sedimentary Rocks		
Sandstone	8 – 4 x 103	2.5 x 10-4 - 0.125
Shale	20 – 2 x 103	5 x 10-4 – 0.05
Limestone	50 – 4 x 102	2.5 x 10-3 – 0.02

Soils and Waters		
Clay	1 – 100	0.01 – 1
Alluvium	10 – 800	0.02 1.25 x 10-3 – 0.1
Groundwater(Fresh)	10 – 100	0.01 0.1
Sea Water	0.2	5
Chemical		
Iron	9.074 x 10-8	1.102 x 107
0.01M Potassium Chloride	0.708	1.413
0.01M Sodium Chloride	0.843	1.185
0.01M Acetic Acid	6.13	0.163
Xylene	6.998 x 1016	1.429 x 10 -17

2.3. Principles of Electrical Method

The fundamental principle behind collection and interpretation of electrical resistivity measurements originate in the electrical physical theory of Ohm's law. Ohm's law states that the product of the electrical current, I, through a conductor and the resistance of the conductor, R, for which the current passes, is equivalent to the potential difference, V, across the conductor(Loke,2000). This is expressed in equation (2.3)

$$V = IR \tag{2.3}$$

We can therefore define resistivity of a material as the resistance in ohms between the opposite faces of a unit cube of the material (Figure 2.1). The units for electrical potential, current and resistance are volts, amperes, and ohms respectively.

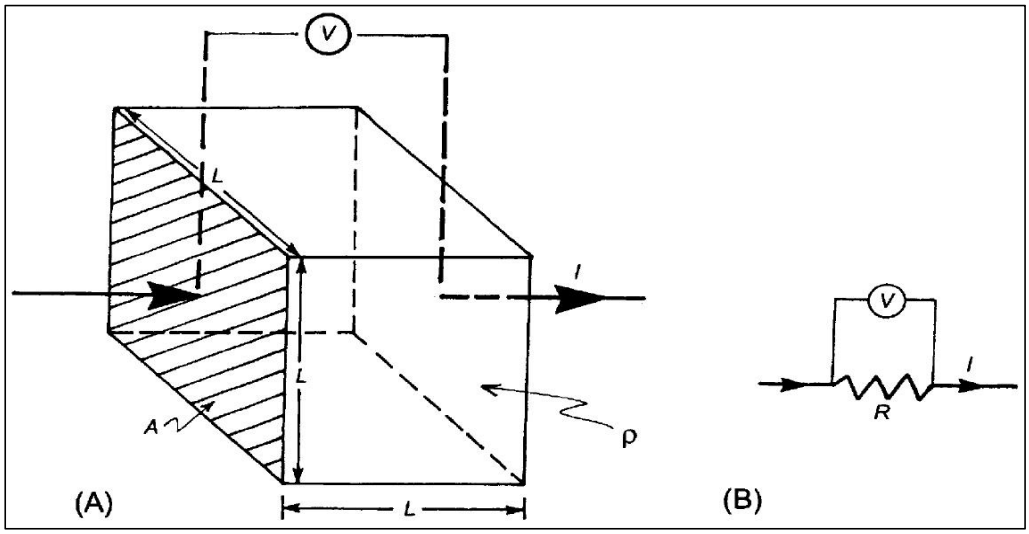

Figure 2.1: Parameters used in Defining Resistivity (Reynolds, 1997).

Where A= Cross Sectional Area, L=Length of Wire, I= Current, R= Resistance, ρ= Resistivity, V= Potential Difference.

To further explain and have better understanding of the principle of electricity, let us consider current I flowing through a wire of length L and cross sectional area A as shown in Figure 2.1. The resistance R, of the wire can be expressed in terms of A and L as shown in equation (2.1) (Reynolds, 1997).

$$R \propto \frac{L}{A}$$

(2.4)

The constant of proportionality is resistivity given as (ρ).Thefore, the total resistance of the wire element, R, is the product of the material resistivity, ρ, and the ratio of the wire length and cross-sectional area as illustrated in the relationship above. It follows that ;

$$R = \rho \left[\frac{L}{A}\right]$$

(2.5)

Considering the physical relationship between the geometry of the conductor and the materialproperty, equation (2.4) can be manipulated to determine the material resistivity of the conductorelement as expressed in equation (2.5).

$$\rho = \mathrm{R} \left[\frac{A}{L}\right]$$

(2.6)

This form states that the units for resistivity are dependent on the volume of space for which the current travels. The SI unit of resistivity is the ohm-metre (Ωm) and the reciprocal of resistivity is termed conductivity (units: Siemens (S) per metre; $1Sm-1 = 1\Omega^{-1}m^{-1}$) (Kearey *et al.*, 2002).

2.3.1 Theory on Electrical Resistivity Survey

Considering a current flow in a homogeneous Earth, the measurement of potential difference can be related to the dissipation of electrical current within an infinite, homogenous half-space. In this scenario, the application of an electrical current travels in radial fashion out from the point of origin (Figure 2.2). During the current application, the resistance at any location away from the point of origin within the homogeneous mass can be found by determining the radius from the point of origin and the surface area of the respective hemispherical equi-potential surface.

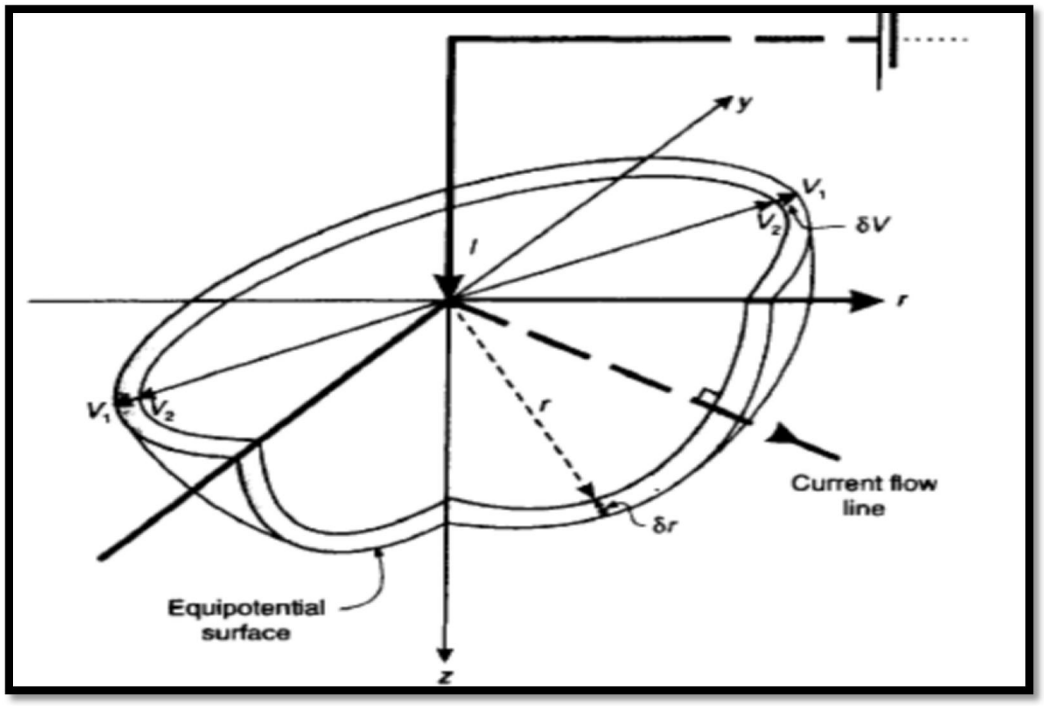

Figure 2.2: Three-Dimensional Representation of a Hemispherical Equi-potential Shell around a Point Electrode on a Semi-Infinite, Homogeneous Medium (Reynolds, 1997).

Relating this model to the original example, equation (2.4) can be rewritten using the radius, r, as the distance for which the current travels and the surface area of the resulting equi-potential surface, $2\pi r^2$ (i.e. r = L and A = $2\pi r^2$). Equation (2.6) describes the system resistance at any point away from the point source, within the homogeneous mass.

$$R = \rho\left[\frac{r}{2\pi r^2}\right] = \frac{\rho}{2\pi r}$$

(2.7)

Next we try to relate Ohm's Law to the resistance of the semi hemispherical homogeneous earth model. Recall, Ohm's Law state that V= IR, substituting equation (2.6) into equation (2.3) will give the potential difference as shown in equation (2.7).

$$V = IR = I\left[\frac{\rho}{2\pi r}\right]$$

(2.8)

Likewise, the potential difference between any two points within the homogeneous mass would be the difference between the two equi-potential surfaces, as expressed in equation (2.8) (Gibson *et al.*, 2003).

$$V = \left[\left(\frac{\rho}{2\pi r_1}\right) - \left(\frac{\rho}{2\pi r_2}\right)\right]\left(\frac{I\rho}{2\pi}\right)\left[\left(\frac{1}{r_1}\right) - \left(\frac{1}{r_2}\right)\right]$$

$$\therefore \rho = \left(\frac{2\pi V}{I}\right)\left[\frac{1}{\frac{1}{r_1} - \frac{1}{r_2}}\right]$$

(2.9)

Equation (2.8) relates the applied current, I, and measured potential difference, V, to a constant value which accounts for spatial considerations, or the way in which the reading was acquired. In a homogenous media, the measured resistivity will be equivalent to the true value of resistivity at a given location with the media. However, the occurrence of a homogenous condition is rare, if not non-existent in practice. In order to account for the inherent heterogeneity of the earth, a collected reading is considered an apparent resistivity measurement. Now considering a source and sink points at the surface of the earth (Figure 2.3).

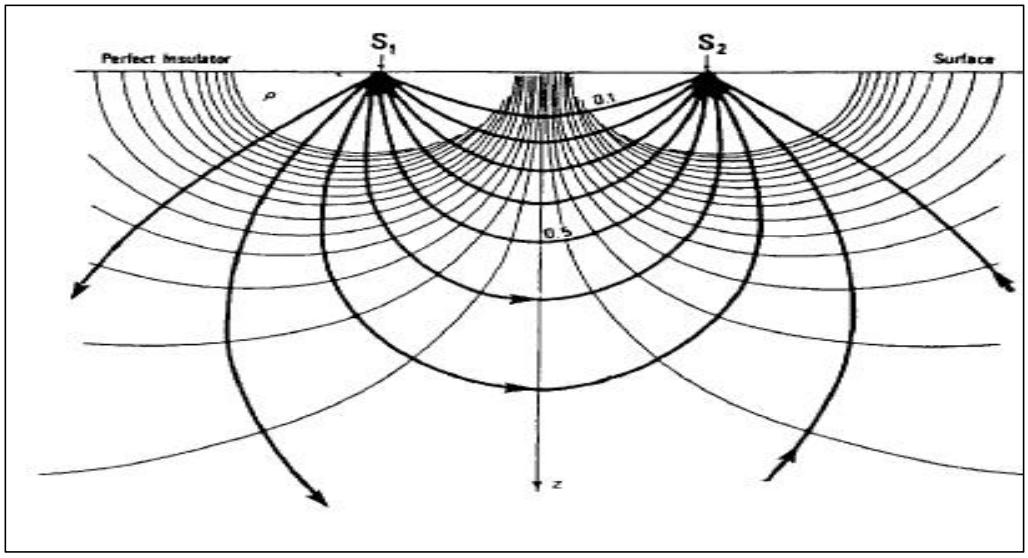

Figure 2.3: Current and Equi-potential Lines Produced by a Current Source and Sink (Reynolds, 1997).

and applying equation (2.7), a point source potential will be established as expressed in equation (2.9):

$V = \left(\frac{\rho I}{2\pi r}\right)$ (Reynolds, 1997)

(2.10)

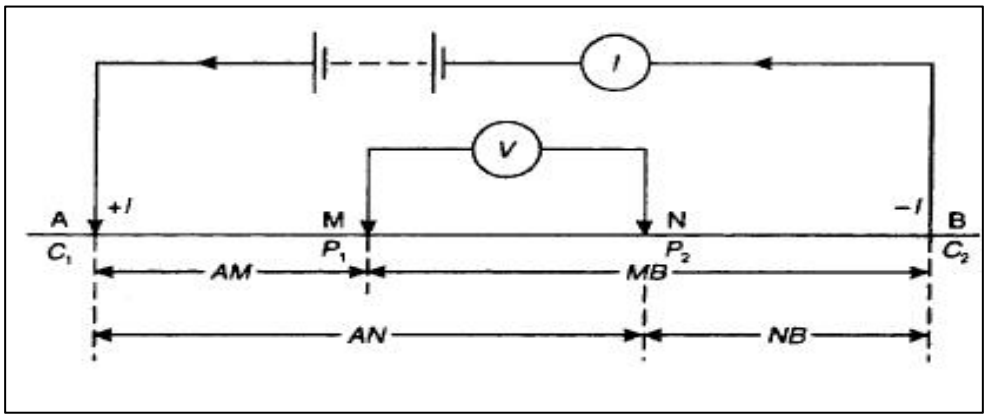

Figure 2.4: Generalized Form of Electrode Configuration in Resistivity Surveys (Kearey et al., 2002).

Equation (2.6) can be used to derive the potential derive from a source and sink sources. For a current source and sink, the potential V_p at any point P in the ground is equal to the sum of the voltages from the two potential electrodes.

The potentials at electrodes M and N from Figure (2.4) are illustrated in equation (2.10):

$$V_M = \frac{\rho I}{2\pi}\left[\frac{1}{AM} - \frac{1}{MB}\right], V_N = \frac{\rho I}{2\pi}\left[\frac{1}{AN} - \frac{1}{NB}\right]$$

(2.11)

To measure the potential difference ΔV_{MN}, equation (2.10) can be rewritten as expressed in equation (2.11):

$$\Delta V_{MN} = \Delta V_M - \Delta V_M = \frac{\rho I}{2\pi}\left[\frac{1}{AM} - \frac{1}{MB}\right] - \left[\frac{1}{AN} - \frac{1}{NB}\right]$$

(2.12)

This can be rearranged making resistivity (ρ) the subject of the formula as illustrated in equation (2.12) Reynolds, 1997.

$$\rho = \frac{2\pi\Delta V_{MN}}{I}\left\{\left[\frac{1}{AM} - \frac{1}{MB}\right] - \left[\frac{1}{AN} - \frac{1}{NB}\right]\right\}\text{-}1$$

(2.13)

However $\left\{(2\pi)\left[\frac{1}{AM} - \frac{1}{MB}\right] - \left[\frac{1}{AN} - \frac{1}{NB}\right]\right\}\text{-}1 = K$

$$\therefore, \rho_a = \left(\frac{V}{I}\right) k$$

(2.14)

where K is the geometric factor and ρ_a is the apparent resistivity. It is worth nothing that K varies with different arrays (Kearey et al., 2002). The spacing and layout of current and potential electrodes impacts the induced equipotential fields generated within the earthen mass. Note resistivity (ρ) is now apparent resistivity (ρ_a). This is as a result of inhomogeneity of the ground. Field measurements taken are apparent resistivity while resistivity realized from interpretation of field data is real resistivity.

2.4 Types of Resistivity Surveys.

The most common electrical methods used in hydrogeological and environmental surveys are Vertical Electrical Soundings (VES) and Horizontal Electrical Profiling (HEP). Horizontal Electrical Profiling is used for assessing lateral variations and vertical electrical sounding is

used for investigating depth. The basic difference between these two aspects of measurements is that in profiling measurements are taken at various stations on the profile. Another improvement in the electrical methods is the 2-D electrical imaging method. This method takes care of the resistivity changes in both the vertical direction as well as the horizontal direction along the survey line.

2.4.1 Vertical Electrical Sounding (VES)

Vertical electrical sounding (VES) consist of a symmetric geoelectrical array that can be used to determine the electrical resistivity of the subsurface (Ledo, 2007). The objective is to deduce the variation of resistivity with depth below a given point on the earth surface and to correlate it with available geological information in order to infer the depth and resistivities of various layers. The measurements are taken by gradually increasing the current electrode spacing with the potential electrode spacing constant at some stations.

The wider the current electrode spacing, the deeper the current penetrates thereby increasing the depth of investigation. When sounding over a relatively homogeneous half-space, the separation between transmitter and receiver should be about five times the depth of investigation. This implies that, if you want to see down 2km, the receiver- transmitter separation should be 10km (Zong, 1992).

2.4.2 Horizontal Electrical Profiling (HEP)

The aim of HEP is to detect lateral differences in the resistivity of the subsurface. Profiles make use of fixed electrode spacing, and the mid-point of the electrode spread is moved for each reading (Exploration Geophysics, 2002). The entire changes of resistivity at each stations are used to select anomalous stations for further investigations or drilling (Ewusi, 2006).

2.4.3. 2-D Electrical Imaging Method

Two-dimensional resistivity measurements give a two-dimensional vertical picture of the sounding medium. The current and potential electrodes are placed at a regular fixed distance from each other and are progressively moved along a line on the earth surface. At each step, one measurement is recorded. The set of all these measurements at this first inter-electrode spacing gives a profile of resistivity values. The inter-electrode spacing is increased by a factor n = 2 and a second measurement line is carried out. This process of increasing the factor n is repeated until the required spacing between electrodes is achieved. An increase in the distance between two electrode pairs gives the apparent resistivity at greater depths (Figure 4). Howbeit, current distribution in the subsurface is a function of resistivity contrasts of the different media and the depth of investigation gotten from the electrode spacing is called the "pseudo-

depth''. The data are then arranged in a 2D pseudo-section plot that gives both horizontal and vertical variations in resistivity display simultaneous (Samouelian et al, 2007).

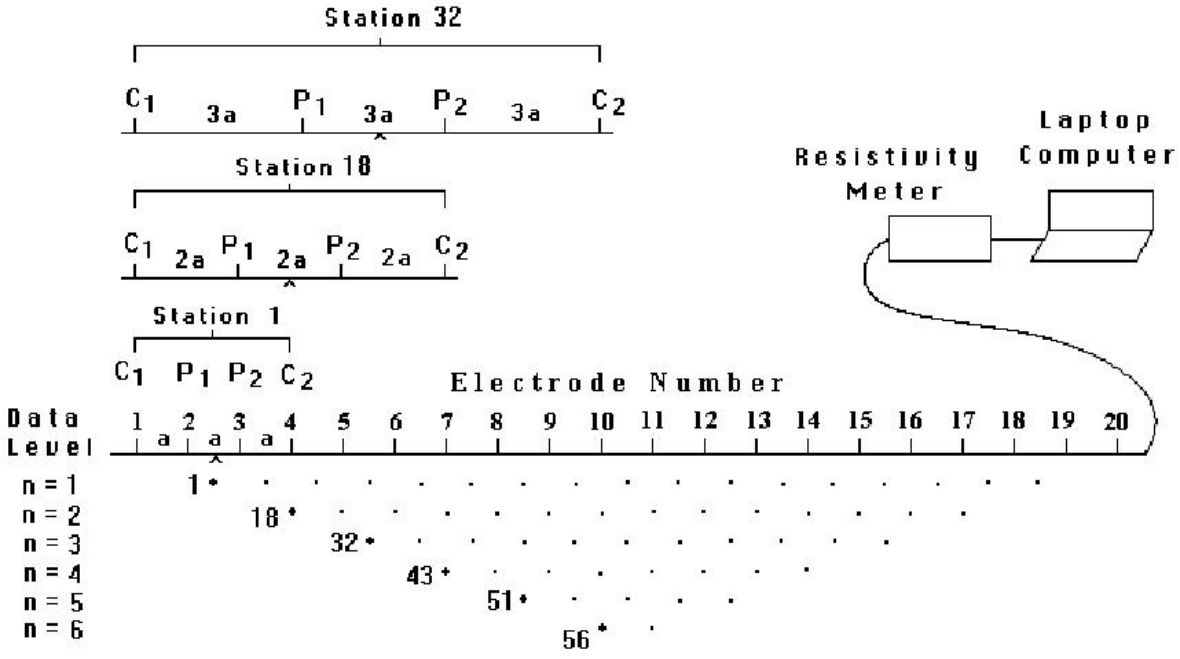

Figure 2.5: Construction of pseudo-section for Wenner resistivity data (Loke, 2001).2.5 Electrode Configurations

2.5.1 Wenner Array

Wenner array is broadly used, and supported by many interpretational literature and computer packages. It is the 'Conventional' array against which others are often assessed. Figure

2.5 shows a pictorial representation of Wenner array and its geometric factor.

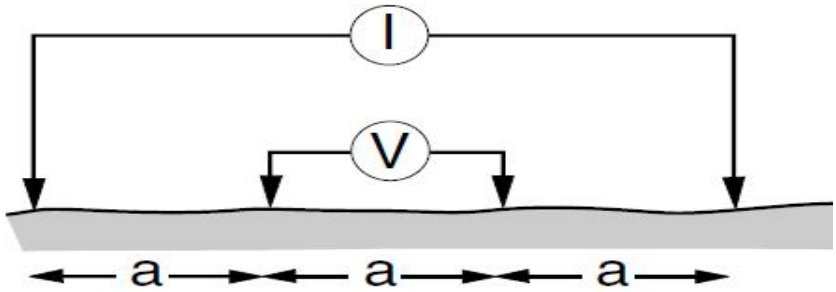

Figure 2.6: Wenner array and its geometric factor (Milsom, 2007)

2.5.2 Schlumberger Array

Schlumberger array: the only array that contend availability of interpretational material, all of which relates to the 'ideal' array with negligible distance between the inner electrodes. For electrical depth-sounding work, Schlumberger is favoured, along with the Wenner,

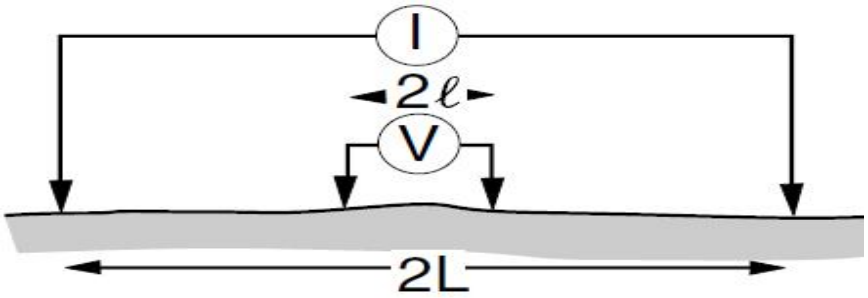

Figure 2.7 Schlumberger Array and its geometric factor (Milsom, 2007)

2.5.3 Pole – Pole Array (Two Electrode)

Two-electrode (pole–pole) array: Theoretically interesting since it is possible to calculate from readings taken along a traverse the results that would be obtained from any other type of array, providing coverage is adequate. However, the noise that accumulates when large numbers of results obtained with closely spaced electrodes are added prevents any practical use being made of this fact. The array is very

popular in archaeological work because it lends itself to rapid one-person operation. As the normal array, it is one of the standards in electrical well logging.

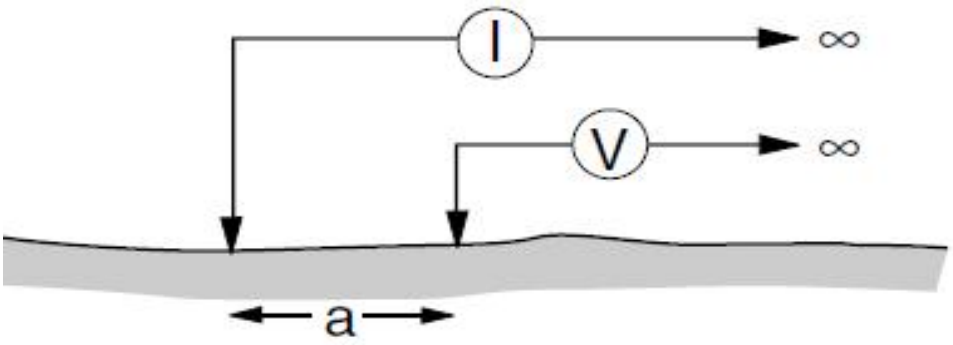

Figure 2.8: Pole – Pole Array (Two Electrode) and its geometric factor (Milsom, 2007)

2.5.4 Pole – Dipole Array

Pole–dipole array: produces asymmetric irregularities that are more difficult to interpret than those produced by symmetric arrays. Peaks are displaced from the mid-poins of conductive or chargeable bodies

and electrode positions have to be recorded with exceptional care. Values are usually plotted at the point mid-way between the moving voltage electrodes but this is not a universally agreed standard. Results can be displayed as pseudo-sections, with depth penetration varied by varying n. Pole-dipole produces low noise ratio as compared to dipole-dipole arrray.(Johnson, 2003).

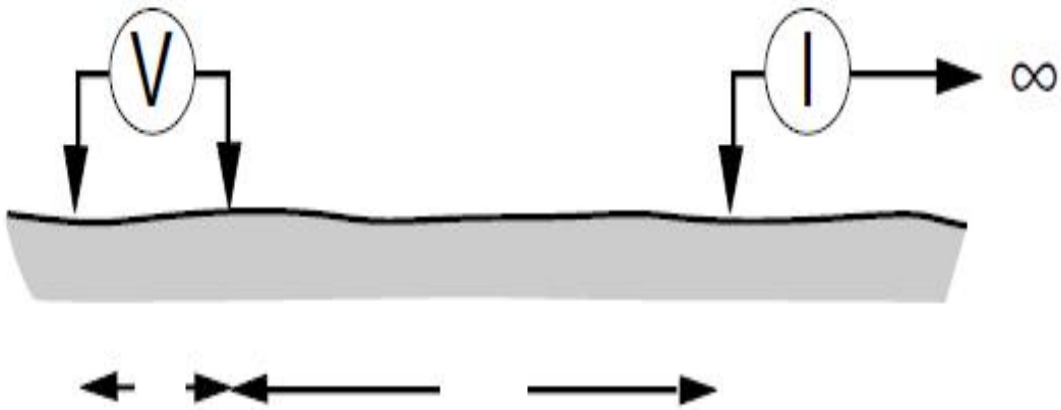

Figure 2.9: Pole – dipole Array and its geometric factor (Milson, 2007)

2.5.5 Dipole-Dipole Array

Dipole–dipole (Eltran) array: popular in induced polarization (IP) work because the complete separation of current and voltage circuits reduces the vulnerability to inductive noise. Dipole–dipole array provides higher and better lateral resolution when compared to Wenner array(Yuen and Sinclair, Evans et al. 1988). It gives room for plotting of raw data in order to get an insight of a cross-section of the earth. Measurement value called apparent resistivity is considered by those that employed the use of dipole-dipole array. Apparent resistivity represnts a weighed average of resistivities under four electrodes used to take the reading. The result plotted from a dipole-dipole survey is Pseudo-section form. It is worthy of note that, for each measurement, the apparent resistivity data is plotted at the mean between the two electrodes and at a depth of one over two of the distance between the two poles. Today,modern inversion software

(Earthimager TM 2D) is capable to convert all of these apparent resistivity values to "true" resistivity values, so that a real image of the ground can be created (Loke 1994).

A considerable body of interpretational material is available. Information from different depths is obtained by changing. In principle, the larger the value of n, the deeper the penetration of the current path sampled. The voltage is inversely proportional to the cube of the "n" factor. By implication, for the same current, the voltage measured by the resistivity meter drops by about 500 times when "n" is increased from 1 to 8. The only way to overcome this short comimgs is to step-up the value of "a' spacing between the curent- current electrode and voltage-voltage electrode dipole pair to reduce the drop in the potential when the total length of the array is increased to increase the deppth of investigation. To effectively use this array, the meter should have high sensitivity, very good noise

rejecton circuitry and the electrodes should be firmly fixed to the earth (avoid loose contact).

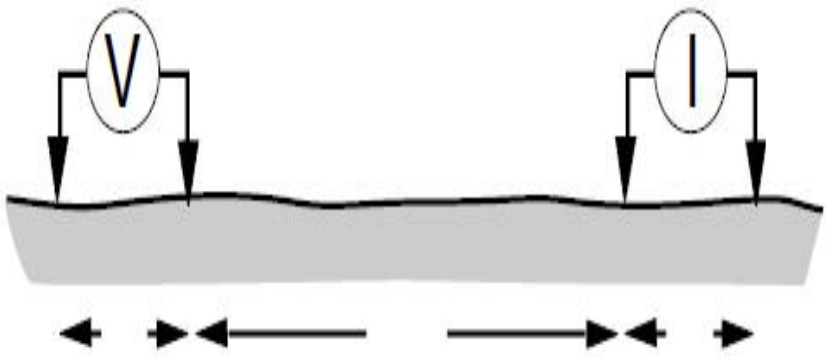

Figure 2.10: Dipole – dipole Array and its geometric factor (Milson 2007)

2.5.5.1 Advantages of Dipole-dipole Array:

i. It has high resolution and multi-channel capability (Griffith et. al. 1990).

ii. It is faster, since it allows multiple measurement to be carried out simultaneously. (The AGI supersting R8 can measure eight simultaneous measurements for each current injection) whereas the Wenner array can only take one data point for each current transmitter insertion.

iii. It is pretty simple to carry out a survey along profile lines using the dipole-dipole array.

2.5.5.2 Shortcoming of Dipole-dipole Array:

The dipoles will dissipate the signal (signal fading) if they are placed too far apart, thereby decreasing the ability to see deeper into the earth.

2.5.6 Gradient Array

Gradient array: popularly used for reconnaissance. Large numbers of readings can be taken on parallel traverses without moving the current electrodes if powerful generators are available.

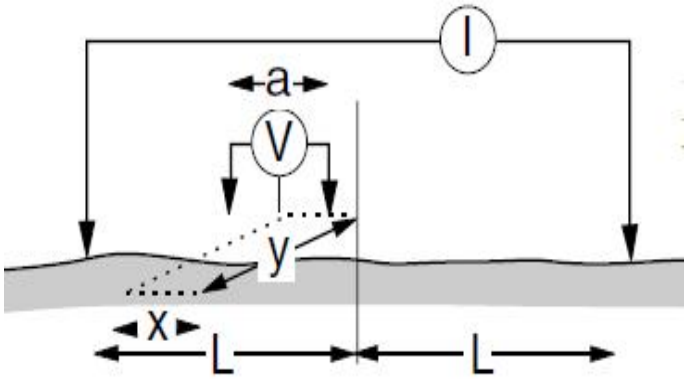

Figure 2.11: Gradient Array and its geometric factor (Milson, 2007

In summary, the higher the value of geometric factor K the lower the voltage value recorded and vice versa. If potental is low, signal to noise ratio will equally be low. Depth of investigation is typically 15-20% of the total spread length (Schlumbeger, dipole-dipole). If the requested depth of investigation is 70m, estimated spread length to 70/0.15=467m(Yuen and Sinclair,2009).

2.7 Limitations of Resistivity Method

Resistivity surveying method is relatively cheap, easy and efficient way of investigation subsurface resistivity, however it does have some limitation, these limitations are:

i. Topography and the effects of near-surface resistivity variations can mask the effects of deeper variations.

ii. The depth of penetration of the method is limited by the maximum electrical power that can be introduced into the ground and by the physical difficulties of laying out long lengths of cable. The practical depth limit for most surveys is about 1km.

iii. Interpretations are ambiguous. Consequently, independent geophysical and geological controls are necessary to discriminate between valid alternative interpretations of the resistivity data.

iv. Interpretation is limited to simple structural configurations. Any deviations from these simple situations may be impossible to interpret (Kearey *et al.*, 2002).

v. In depth sounding, resistivity resolution reduces with increasing depth.

vi. The most severe limitation of the resistivity sounding method is that horizontal (or lateral) changes in the subsurface resistivity are commonly found. Lateral changes in the subsurface resistivity will cause changes in the apparent resistivity values that might be, and frequently are, misinterpreted as changes with depth in the subsurface resistivity (Loke, 2000).

CHAPTER THREE

METHODOLOGY

3.1 Introduction

The advancement in the development of microcontroller technology, high speed digital signal processing, wireless communication system technologies and the benefits attainable have necessitated the upgrades in the system designs and implementation that can meet up with the timely demand for reliability and convenience. The use of internet of things (IOT) for the wireless communicationis for data collection,transmission and cloud storage in difficult terrain condition and other places that are difficult for people to reach (Aravinth. et al; 2018). The design of the Terrameter undertaken in this design is presented under three main sections namely; Materials and methods, Hardware design and software design.

3.2 Materials and Methods

The system has the following parts; DC power source, high DC voltage generator unit, measurement unit (current and voltage measuring unit), processing unit (Arduino Nano), transmission unit (GSM Modem) and IOT cloud service (Thingspeak data acquisition and cloud storage). This is as shown in figure 3.1 and this doubles as the flowchart of system development.

3.2.1 DC Battery

The power source foe the system is from a 12V, 7AH battery source.

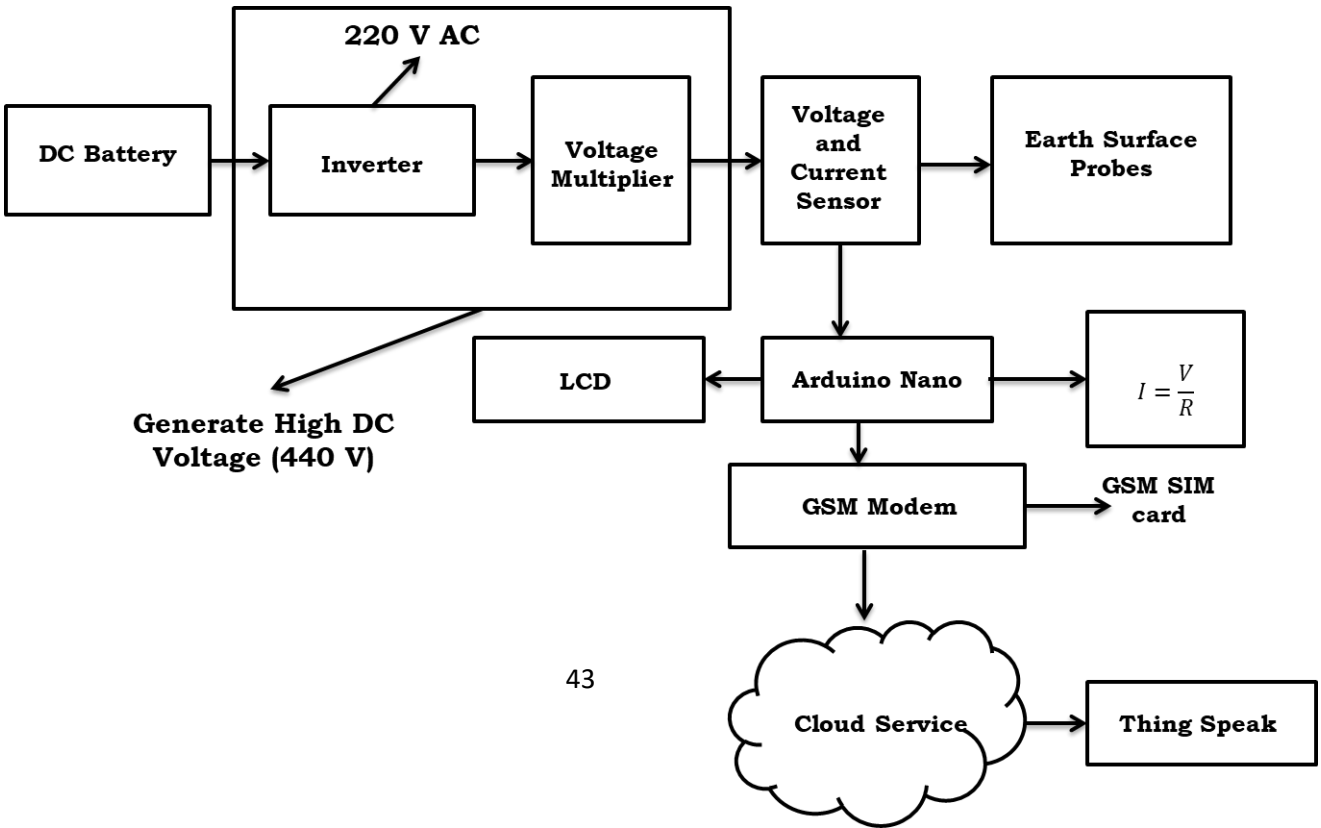

This was used so that the system would portable and has enough power for testing. testing.

Figure 3.1 Block diagram of Flowchart showing the Design and Development Process for a Wireless Resistivity Meter

3.2.2 High DC Voltage generator

This stage generates high DC voltage of 440V for the probes, enough to cause current flow and potential difference development across measuring points on the earth surface. It consists of an inverter and a voltage multiplier circuit.

3.2.3 Voltage and Current Sensing circuit

This section has the sensor circuit that measures the voltage across the probes on the earth surface and the current through the earth crust.

3.2.4 Transmission unit

The transmitting unit is for communication between the system and the IOT cloud server hosting the IOT cloud service. A SIM800L gsm module was used for the data transmission.

3.2.5 Display Unit

This is the display on ground for monitoring the measurement data generated. The display used is the liquid crystal display

3.2.6 Processing unit

This stage handles the processing of the voltage and current data into digital format for driving the gsm module. It is made up of Arduino Nano module. It uses Atmaga328Pmicrocontroller. Figure 3.4 shows the pinout of ATMEGA328P. It has 1KB Electrically Erasable

Programmable Read Only Memory (EEPROM). This property indicates if the sources of power to the micro-controller is removed, even then it can store the data and can provide results after providing it with the electric supply. Moreover, ATmega328 has 2KB Static Random-Access Memory (SRAM). ATmega328 has several different features which make it the most unique device in today's electronic market. These features include cost efficiency, low power dissipation, programming lock for security purposes, real timer counter with separate oscillator, advanced RISC architecture, good performance, real timer counter having separate oscillator, 6 PWM pins, programmable Serial USART, programming lock for software security, throughput up to 20 MIPS etc. ATmega328 is mostly used in Arduino.

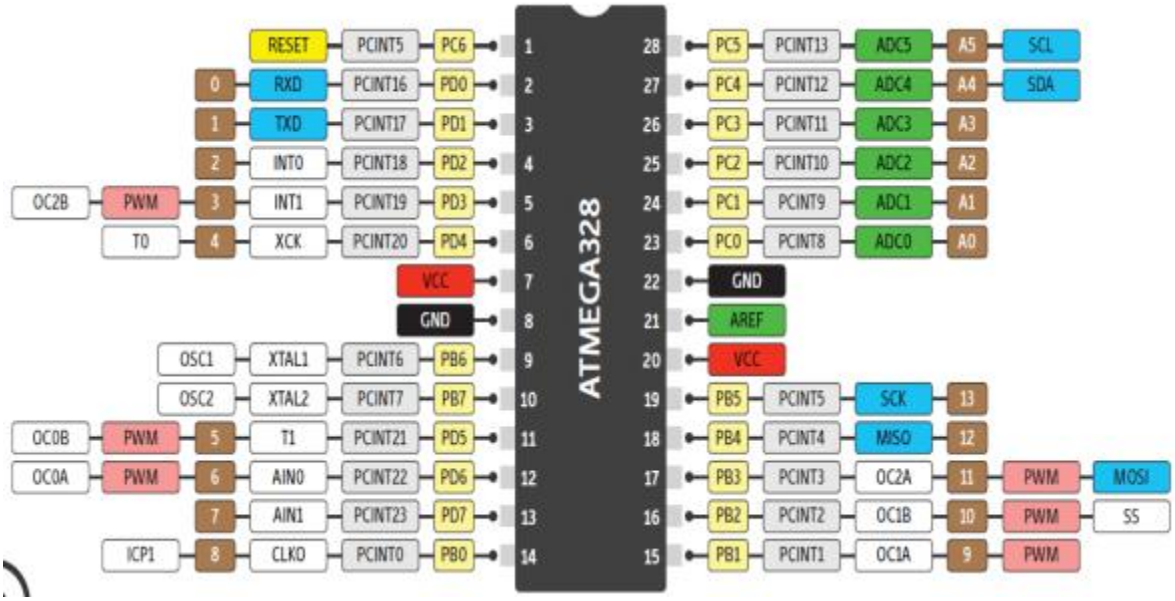

Figure 3.2: Pinout of ATMEGA328P.

3.3 Hardware Design analysis

This section presents the hardware design analysis of the system involving the high dc voltage source, voltage and current sensor and transmitting unit.

3.3.1 Design Of Pulse Width Modulator

The pulse width modulator stage is designed using a dedicated PWM IC, **SG3524**.This versatile PWM controller can be used in a variety of

isolated and non-isolated switching power supplies such as inverters.

The figure 3.3 shows the pin configuration of the chip.

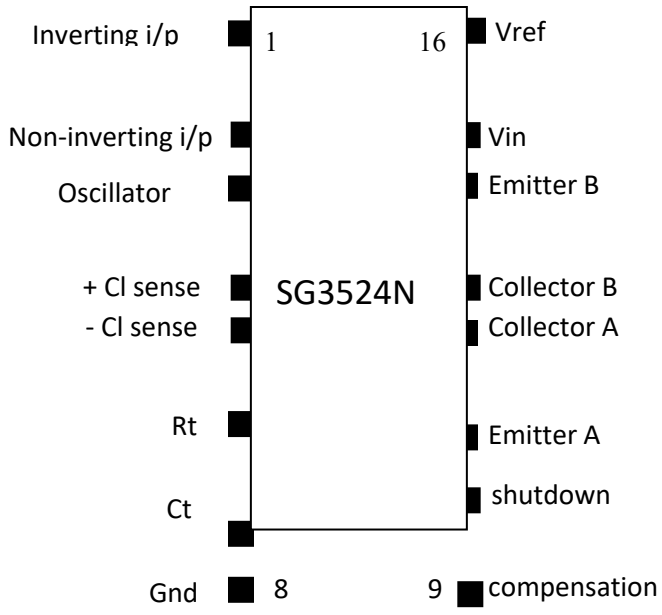

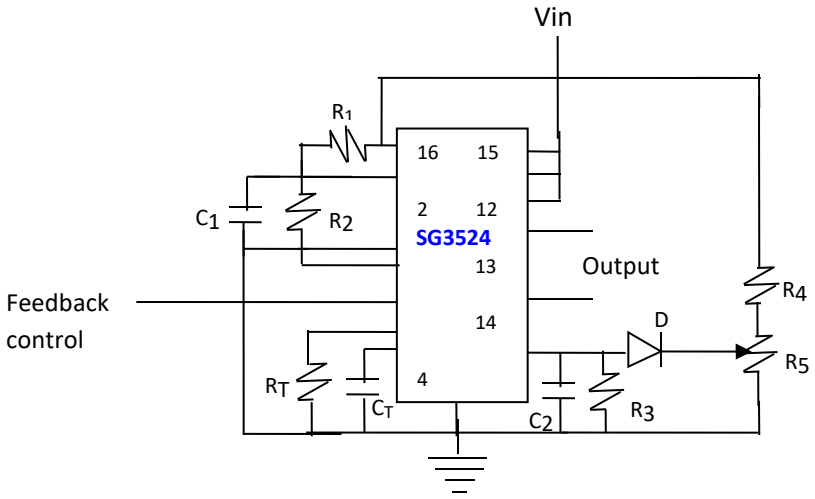

Figure 3.3 Pin configuration of SG3524 PWM IC and circuit

Define the frequency of Oscillation, fr $= \frac{1.15}{2R_T C_T}$ = 50Hz

- Choosing C_T = 0.2μF
- $R_T = \frac{1.15}{2FC_T}$

$= \frac{1.15}{2x50x0.2x10^{-6}}$ = 57500Ω = 57.5KΩ

- Battery voltage is 12V d.c.
- A fixed value of 56KΩ and a variable resistor, which is adjusted to 20KΩ, was used in the design.

- VIN for the PWM IC is taken from the battery source.
- The chip is powered with 12 volts through a 7812 voltage regulator.
- Pin 16 is connected to an internal +5V regulator and it was used to set the voltage reference of 2.5V for the pulse-width control through voltage divider resistors to pin1. From voltage divider theory both resistors value are equal and recommended value for R1 and R2 resistor according to datasheet is 5kΩ but 4.7kΩ was used as the closest available standard value. C1 was connected for stability and its chosen value is 47µF.
- Pin1 was used as the feedback control input form the Optocoupler stage.
- C2 and R3 was used for compensation to cancel a pole at frequency,

f = 200Hz as recommended by the datasheet for stability and their values can be determined from the expression;

$F = 1/RC$

Choosing C2 = 100nF, $R = (FC)^{-1} = (200 \times 100 \times 10^{-9})^{-1}$

R3 = 50,000Ω

A value of 47kΩ was used as the available standard.

Resistors R4 and R5 form a voltage divider to aid manual pulse-width variation through compensation pin. The recommended control voltage maximum is 3.4V. To achieve this R4 is fixed while R5 was made variable for pulse-width adjustment. According to voltage divider theory,

$Vo = Vin\ [R5 / (R4 + R5)]$ and reference voltage Vin = 5V and thus;

Choosing R4 = 4.7kΩ,

$R5 = R4\ [Vo / (Vin - Vo)] = 4700[3.4 / (5 - 3.4)]$

$R5 \approx 10k\Omega$

Diode D2 was connected to prevent R4 and R5 from affecting the compensation by R3, C2.

3.3.2 Design Of Mosfet Driver

The MOSFET stage conducts the necessary load current through the step up transformer.

- The MOSFET used in the design is the ***IRFZ44N-channel.***
- Fixed resistors of 10kΩ were connected between the gate and source to aid fast switching by discharging any residual static charge at the gate.

IRFZ44N DATA

Drain to source breakdown voltage BV_{DSS}= 60V

Gate to source voltage (cut-off) = 4V

Gate to source breakdown voltage = ±20V

Drain current (continuous) = 30A

Drain to source resistance r_{DSS} = 0.035Ω

Power Dissipation P_D = 150W

- A total of 4 MOSFET were used for the design of the MOSFET driver. 2 MOSFET function for each half of the full period.

3.3.3 LOW BATTERY INDICATION AND SHUTDOWN

The battery status monitor circuit is designed to give a visual indication using a LED and a buzzer for audio indication of low battery condition during operation. The circuit would delay shutdown of the system after some minutes. The circuit is presented in figure 3.3. The circuit consists of a comparator and a voltage reference set by a zener diode, a passive delay circuit.

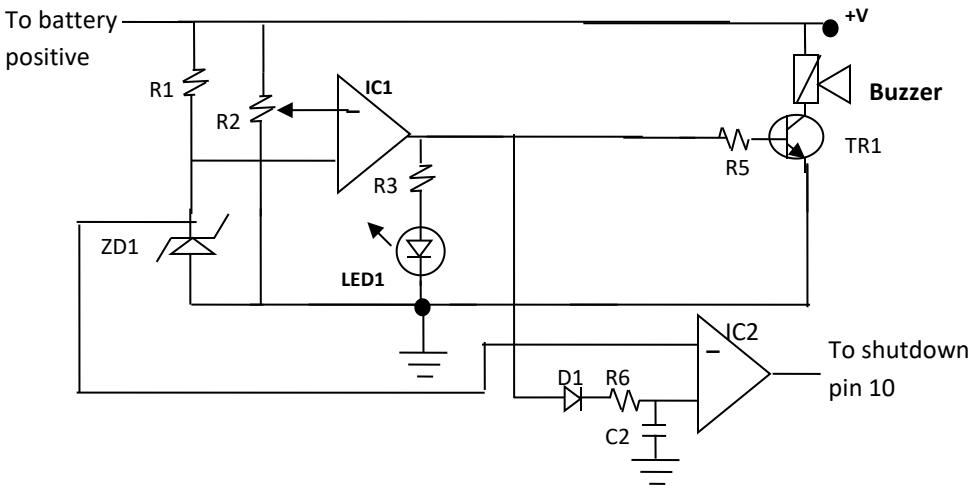

Figure 3.4 Low battery detector and shutdown circuit

A *LM358* op-amp was used for the comparator IC1. it compares the battery charge coupled to it by variable resistor R2. The reference voltage is determined by zener diode ZD1. the zener diode rating is ;

Power rating = 300mW

Breakdown voltage = 6.2V

Thus maximum current $I = P / V = 300 \times 10^{-3} / 6.2 = 48.3$ mA

$R1 = V / I = 6.2 / 48.3 \times 10^{-3}$

R1 = 128Ω

A value of 120Ω was chosen as closest standard value.

IC2 and R6, C2 and D1 form a passive delay circuit. The function is to create delay before shutdown from the time low battery charge is detected to when the inverter shuts down. Diode D1 prevent C2 from discharging into IC1.

Time delay $\tau = 0.7R_6C_2$

For a minute delay T = 60s and C_2 = 100μF

$R_6 = 60 / (0.7 \times 100 \times 10^{-6}) = 857142\Omega \approx 1M\Omega$

The limiting resistor value for the LED can be determined thus,

$$R_3 = \frac{V_{cc} - V_f}{I_F}.$$

Where R_L = Limiting resistance

I_F = Forward conducting current

V_F = Forward voltage drop

V_{cc} = Comparator Output

For the LED, V_F = 2.2V, I_F = 8mA, V_{cc} = 9V

$$R_3 = \frac{9-1.8}{8x10^{-3}} = 850\Omega$$

A value of 820Ω was used in the design as the closest standard.

Tr1 is the buzzer driver and it is enabled whenever there is an output from IC1 indicative of a low battery condition. R5 is a base resistor.

For a base current of 1mA, the resistor

R_7 = (Vcc – Vbe) / I

Where I = base current

Vcc = supply Voltage of 12V

R_5 = (12 – 0.6) / 1 x 10^{-3}

R_5 = 11.4kΩ

A value of 10kΩ was chosen as the standard value.

3.3.4Changeover Switch

An automatic changeover switch was designed for this project to aid for battery charging when the battery is down and plugged into utility power.

- A 220Volts operating relay was connected to serve as the mains voltage detector and switchover. When mains power is interrupted this activate relay switch contact to change over the supply from mains to inverter mode supply.
- The action reverses when mainspower is restored, hence providing automatic changeover action.

3.3.5 Optocoulpler Feedback

The optocoupler is used in the feedback loop to control the pulse width, thereby effecting voltage regulation.

- The optocoupler used in the design is the4N35.Tthe chip is as shown below

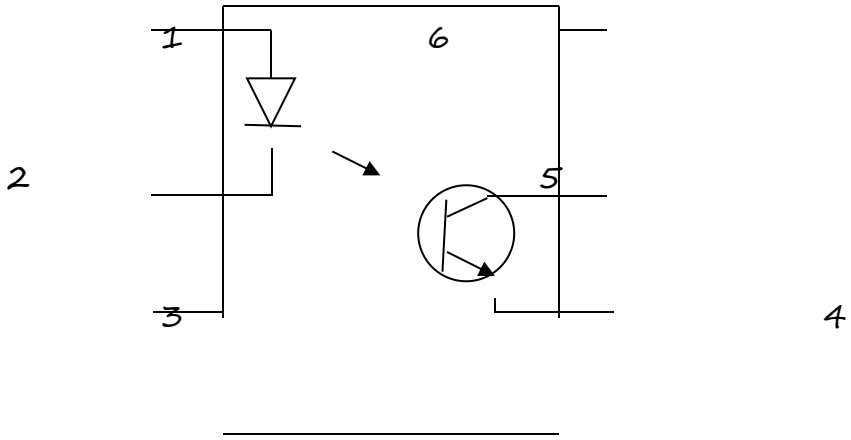

Figure 3.5 Pin configuration of the 4N35 optocoupler

- The LED has a forward current of 5mA and the photo transistor has a maximum current of 200mA.

- A bridge rectifier provides dc input to the LED of the optocoupler.
- For a conducting current of 1mA, the. limiting resistor would be:

$R = \frac{V_s - V_f}{I_F}$ for V_s = 220V, V_F = 2V, I_F = 1mA

$= \frac{220 - 2}{1x10^{-3}} = 218000\,\Omega$

= 220kΩ

- For the pulse width control, the pin 2 is used for the reference voltage.
- Using a voltage divider of equal resistance, the V_{ref} for pin 2 be set to 2.5V when the supply is taken from pin 16 V_{ref}.
- Choosing R_1 and R_2 to be 10KΩ, this implies then that for a collector current of 1mA in the photo transistor, the resistance R_E needed will be;

$$R_E = \frac{V_{refe}}{I_c} = \frac{2.5}{1x10^{-3}} = 2500\,\Omega$$

Thus a variable resistor of 5K Ω was used and adjusted accordingly.The feedback control is as shown figure 3.5. The diode used has a PIV of 400V.

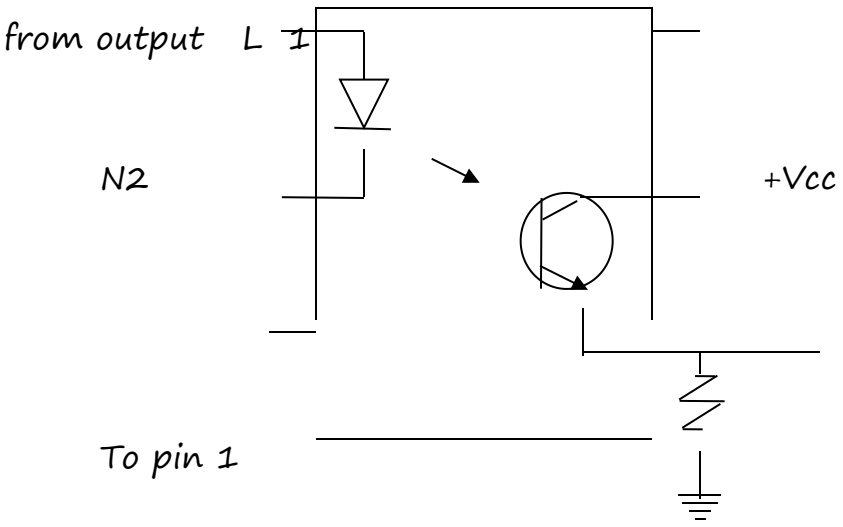

Fig. 3.5 Optocoupler feedback control circuit

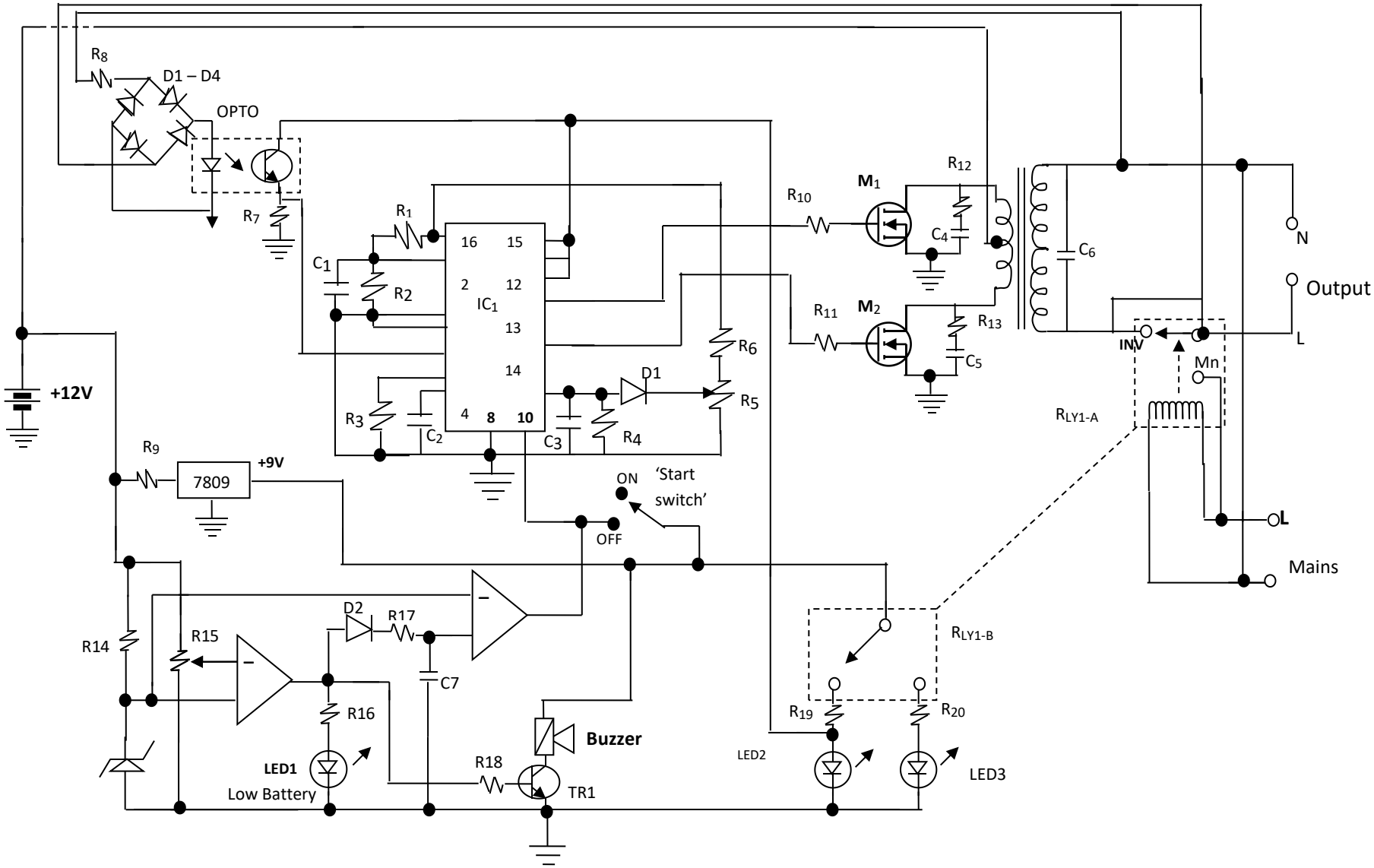

Figure 3.6 Complete circuit diagram of the High DC generator circuit

3.3.6 Operational Principle Of The High Dc Voltage Generator

IC1 is the pulse-width modulator and its function is to generate the $50H_Z$ alternate pulses needed to drive the mosfets. R_4 and C_3 are for compensation while R_3 and C_2 determine the frequency of oscillation. R_1 and R_2 set the Reference voltage of 2.5V for pulse-width modulation control through pin 2 of IC1. This reference is constantly compared with the voltage at pin 1 from the opto-coupler to determine the trend of the pulse-width variation but it works in inverse relation as to balance the change in output voltage such that when the output voltage tend to increase, the pulse-width reduces and vice-versa to keep the output voltage constant within a tolerance range.

Mosfet M_1 and M_2 make up the power drivers. The alternate pulse output from IC1 is fed to mosfets M_1 and M_2. M_1 and M_2 switch the d.c voltage at the primary of transformer T_2, which is serving as the step-up transformer, to create the alternating voltage (a.c) effect and flux change

needed for transformation by the transformer. The transformer then would step-up the now converted 12Vdc to 12V a.c to 220V a.c.

Opto-coupler, bridge rectifier D_1-D_4, C_8, R_7 and R_8 make up the feedback network.. The output voltage is rectified to d.c and slightly filtered by C_8 . R_7 helps for fast discharge of C_8 for effectiveness in tracking output voltage change. Resistor R_8 function is for appropriate adjustment of the error voltage for effective control. The source of the feedback voltage is taken from the output of the auxiliary winding. When the output voltage increases, the auxiliary winding (Aux) output voltage increases and this causes increase in output from R8. This change is detected by IC1 through pin1 and the consequence is that the pulse-width of the pulses generated is gradually reduced in proportion to the change. This is such so that the output voltage that was initially high would begin to drop to the nominal value and vice-versa.

The other stages are the supervisory stage. They consist of the low battery charge detection and switch/changeover stage.

The changeover switch is the Relay. The coil of the relay serves as the mains voltage detector as it energizes when there is mains supply. The Relay controls the load (output) to mains supply whenever mains supply is restored. IC1 is instantly shutdown by cutting off power to it by relay RLY-2 switching contact.LED3 comes on to indicate mains supply while LED2 indicate inversion.

The shutdown of IC1 stops inversion process. This inversion stoppage enables the transformer to now function as a step-down transformer (T_2), stepping down 220V from mains to 12Va.c which is then rectified to d.c by mosfets M1 and M2 which will now serve as diodes to charge-up the battery.

The next supervisory circuit is the low battery charge detector. IC2 is a comparator that detects the low battery charge of 10V by comparing a

sampled d.c charge voltage from the battery through R_{13} and a reference voltage set by zener diode Z_{D1}. When the low charge limit is reached (which is at 10V), the comparator output goes positive and LED1 comes on to indicate low battery charge.

IC3 and R6, C2 and D1 form a passive delay circuit. The function is to create delay before shutdown from the time low battery charge is detected to when the inverter shuts down. Diode D1 prevent C2 from discharging into IC1.

R_9 is a limiting resistor to 7809 which is a 9V, IC voltage regulator.

R_{12} = limiting resistance to Zener diode (ZD1)

R_{14} R_{17}, R_{18} = limiting resistances to LED_S.

M_1 and M_2 represents bank of 8 Mosfets connected in parallel to handle the load current per each side.

3.3.7 Voltage Multiplier

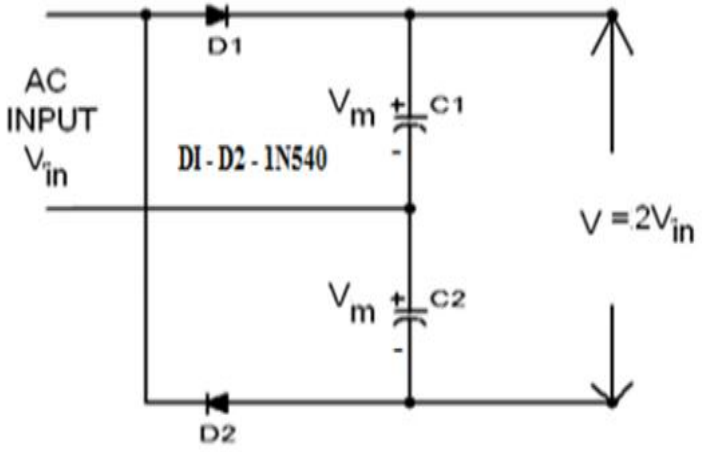

Figure 3.7 Voltage Multiplier Circuit

The half-wave voltage doubler in Figure 3.7, is a multiple of the peak input voltage, the peak input voltage from a supply transformer of rating only Vs max, and each diode in the circuit of PIV rating 2 Vs max. If load is small and the capacitors have little leakage, extremely high dc voltages can be obtained from such a circuit using many sections to step-up the dc voltage. In operation capacitor C1 is charged through diode Dl to a peak value of transformer secondary voltage, Vs max during first positive halfcycle of the ac input voltage. During the negative half cycle capacitor C2 is charged to twice the peak voltage 2 Vs developed by the sum of voltages across

capacitor C1 and the transformer secondary. For this circuit, the 220V ac was rectified to (2Vac) 440V dc.

3.3.8 The Voltage and Current Measuring Unit

The voltage and current measuring unit is monitored by ATMEGA328P microcontroller, the output of the high dc voltage source is fed through a 100 ohm, 5W choke resistor. The voltage developed across the resistor is directly proportional to the current flowing through it. Resistor R1 is the current sensing resistor and J1, J2 are the points for the voltage measuring point from the probes. The analog voltages are fed to the microcontroller that converts the voltages to digital information, processed to drive the GSM module stage. Figure 3.7 illustrate the voltage measuring unit (Transmitter)

3.3.9 GSM Modem stage

The GSM module Unit GSM stands for Global system for mobile. It is a device which modulates and demodulates signals as required to meet communication requirements. It modulates an analogue carrier signal to encode digital information, and also demodulates such a carrier signal to decode the transmitted information. A GSM module is a device that modulates and demodulates the GSM signal and in this particular case 2G signals. The modem used in this study is SIM800L. It is a Tri-band GSM/GPRS modem as it can detect and operate at three frequencies (EGSM 900 MHZ, DCS 1800 MHZ and PCS 1900 MHZ). Default operating frequencies are EGSM 900 MHZ and DCS 1800 MHZ. The figure 3.7 below shows the SIM800L GSM Module. It was used in this work for sake of size and portability as its small size is ideal for the work.

Figure 3.8 GSM modem SIM800L

3.3.10 LCD Display stage

The device uses a 16 × 2 LCD (liquid crystal display) to display the output of the voltage, current and resistivity measurement of the probes during testing activities locally while the information is being transmitted to the IOT cloud service. It is an electronic display module found in wide variety of applications. The 16x2 LCD as shown in figure 3.9 is preferred over seven segment displays and other multi segment LCDs because they are more economical, easily programmable, has no limitations of displaying special and even custom characters and so on. It can display four lines with

maximum of 20 characters per line. In the LCD, each character is displayed in a 5 by 7 pixel matrix.

Figure 3.9 16 x 2 LCD display module3.3.11 Control Program and Software design

The software is designed using arduino IDE specially for arduino based development boards and atmega controllers. The complex and intricate operating routine of the software is achieved by writing sections as demonstrated in the program codes in Appendix A. Arduino IDE (integrated developer environment) was used throughout the software building stage. The software was written in C language and was developed in sections for easy debugging and then later integrated. The integrated program was built and verified and the hex file was generated which was then loaded into the

microcontroller. The flowchart of figure 3.11 shows the code development flowchart.

3.3.12 Internet of Things (IOT) Cloud Service

The cloud service used for this work was the ThingSpeak IOT cloud service. The system is free and good for personal and hobbyist projects. When a user registers with the service, the person can register several channels for data and for this work, the voltage, current and resistivity channels were created so that the data can be transmitted. Each of the channel has a graph that is generated for all data points as it is received from the device at the remote location for testing.After taking data and displaying it, the microcontroller then performs a HTTP push routine to send the data to the internet using the private keys obtained from registration on the Thingspeak cloud web service. The information of the voltage, current abd resistivity are updated on the website automatically. The data can be seen

on the Thingspeak website channel with graph showing the data trend and time stamp.

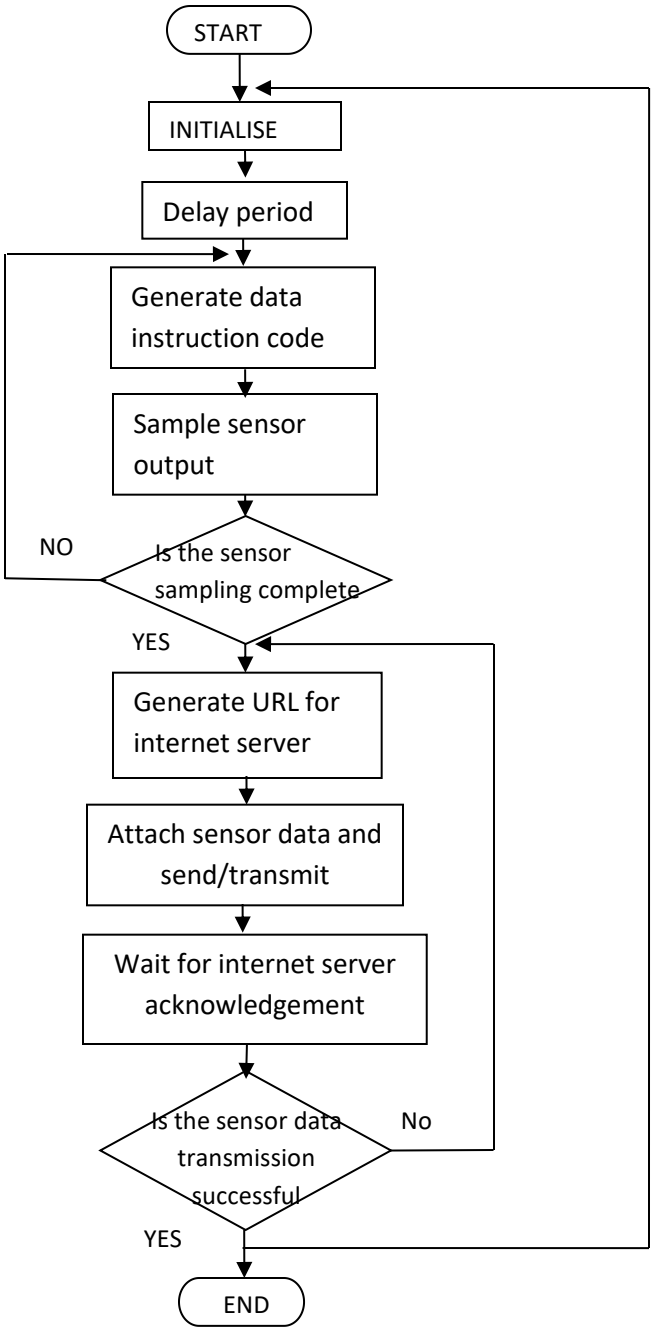

Figure 3.10 Flowchart for codes development for Arduino processor board

CHAPTER FOUR

CONSTRUCTION, TESTING AND RESULT.

4.1 Introduction

This chapter contains an outline of the construction procedure and approach used in this project. Provides description of the steps involved in the construction of each module of the project. The tools and materials used are also stated. The bill of quantities is also presented here.

Modular design approach was used in this project and each module was built and tested separately. This allowed for easy troubleshooting and improved the reliability of the whole system.

4.2 Construction

The construction of the work was embarked on after acquisition of all necessary materials, working tools and components from the market. The construction was done in two phases; first was the breadboard set up. This was necessary so the device can be tested without soldering and easy

adjustment of components to get the best working values. Some of the components were tested to see if they were functional before placing them on the bread board for testing. The second phase was the actual soldering of the components to veroboard for permanent work.

The power supply stage was set up first followed by the microcontroller. The codes for the work was developed using Arduino IDE compiler. After development and debugging of the compiled codes were then downloaded into the microcontroller before the microcontroller was placed on the development board. The high dc voltage sources and the measuring unit stages and GSM module were placed on the board also.

After the test was completed on the breadboard, the components were transferred to a veroboard for permanent soldering. The arrangement also followed the pattern executed on the breadboard. After the soldering work the system was tested and results recorded accordingly.

4.2.1 Tools Used For Construction.

Soldering Iron

Digital Multi meter

Wire cutter

Long Nose Pliers

Razor Blade

Lead Sucker

Stripper

Bread Board

Screw Driver

4.3 General Construction Procedure

4.3.1 Bread board testing.

The first step taking in the construction of this project was to test the design of the circuit on a bread board to see the functionality and performance of the circuit that was designed. Temporary connections using jumper wires are made and different layout of components are tried to reduce the number of connections needed and find the most efficient way to connect the circuit.

4.3.2 Component layout and arrangement.

There were some considerations made during the layout and arrangement of components. First was the access to power and ground. Secondly, the IC's where given priority in terms of arrangement to allow for easy connection to them. Thirdly, input and output leads were taken out from each module

of the circuit. There was always space consideration for the components while being economical as well.

4.3.3 Positioning and soldering of components

Before actual positioning, the surface of the Vero broad was cleared with the sand paper to remove traces of dirt and oxide deposits. Next, the Vero board was broken in to sections for each module of the circuit. Components were positioned according to the flow of the circuit from input to output. Actual soldering was now done ensuring that excess lead does not shut circuit two copper conductors.Short wire leads and were used to interconnect various components and soldering was done as before. Excess or protruding lead of wire and components were cut off and removed. Component leads were joined by ensuring that copper string connecting them were continuous.

They were placed on the project-board and wired together with jumper wires to realize the circuit. The next stage that was set up on the project board was the microcontroller circuit and the transistor relay switches.

The resistors and capacitors were connected as shown by the circuit diagram at the appropriate pin/ports of the ICs. Safety precautions were

observed in the component mounting and connections to prevent short circuit that may arise from wrong component lead placement on the project board.

The program for the microcontroller was developed using Arduino IDE V1.80. The codes were simulated and debugged for errors and those errors found in the course of debugging were corrected.

At completion the machine codes was downloaded into the microcontroller using its USB connection downloader.

The circuit was tested after the whole circuit components have been connected as indicated by the design and circuit schematics, stage by stage to ensure they are working well.

After testing and due adjustment done on it, the circuit components were then transferred to a veroboard for permanent soldering.

The soldering too was done stage by stage to ensure proper connection of parts and wiring. I.C sockets were used for the I.Cs for protection of the I.Cs from soldering iron heat.

The GSM module was connected with appropriate connectors so as to gain access to the receiver Rx and transmitter Tx USART. The soldered terminals were also soldered to the microcontroller pins for Rx and Tx respectively. The following pictures show the circuit stages development

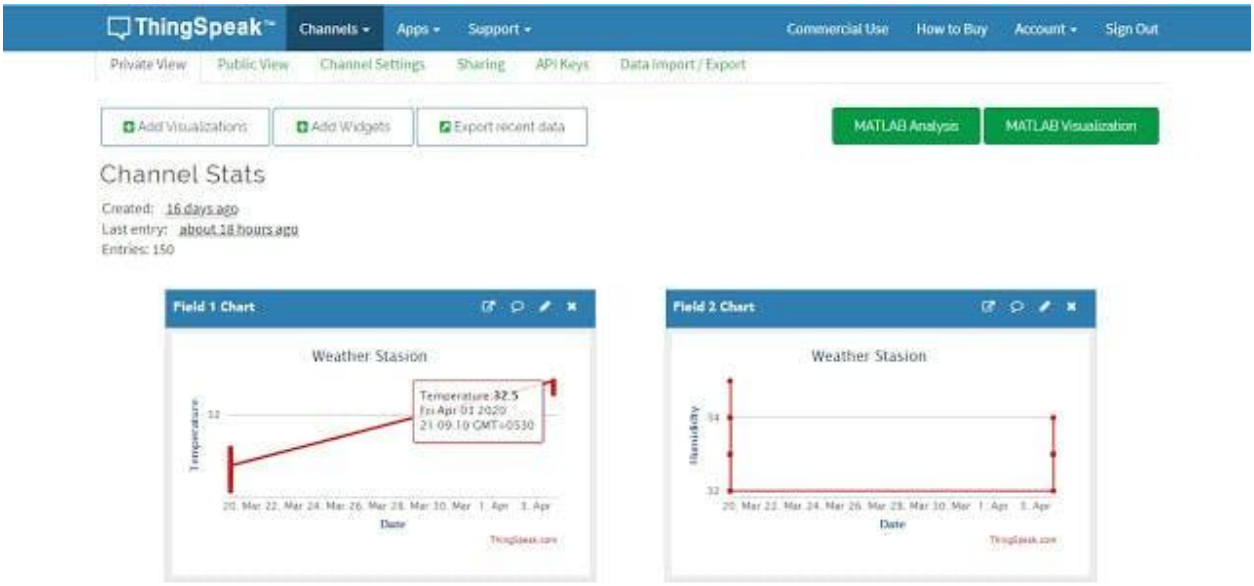

Figure 4.1 Sample of ThingSpeak IOT Web service screen

4.3.4 Casing.

The electronic circuit was enclosed in a Plastic case. The dimensions are as shown in the diagram. The case was designed to suit the purpose of the design.

4.4 Testing and Result

This section shows the test procedures on each stage of the system and also as a complete unit. The tests includes high dc voltage test,voltage and current measurement test, GSM communication test and IOT cloud storage test and complete system test.

4.4.1 High DC voltage test

This test was carried with the help of a digital multimeter with the scale on frequency and voltage ranges. The inverter circuit section was connected to a 12v battery and powered. The frequency of the oscillation was measured, including the ac output voltage and the output of the voltage doubler. These are presented in table 4.1

Table 4.1 Test and result of the high dc voltage generator

S/No	Frequency (Hz)	Output Vac	Voltage doubler output (Vdc)
1	50	223	451
2	52	225	459

4.4.2 Voltage and Current Measurement Test

The test was done after the system was completed and the high voltage dc source was connected to the metallic probes. The ATMEGA328 monitored the voltage and current converted it to digital and then displayed on the LCD screen at different locations. The following table 4.2 presents the test result for voltage and current at different locations.

Table 4.2 Test result for Voltage and Current Measurement

S/No.	Potential Electrode Spacing (L(m)	Voltage (mV)	Current (mA)	Resistance (Ω)
1	0.20	11.32	3.43	3.23
2	0.20	6.64	2.59	2.55
3	0.25	27.39	5.24	5.21
4	0.25	17.41	4.18	4.15
5	0.30	7.31	2.73	2.67

6	0.30	15.72	3.99	3.91
7	0.35	8.87	2.97	2.98
8	0.35	10.52	3.27	3.21
9	0.40	12.31	3.53	3.48
10	0.40	11.46	3.45	3.31
11	0.45	8.52	2.98	2.84
12	0.45	6.21	2.56	2.41
13	0.50	4.95	2.33	2.11
14	0.50	3.679	1.94	1.89

Table 4.3 Test results showing Resistance measurement for different spacing

S/No.	Potential Electrode Spacing (L(m)	Current Electrode Spacing (L(m))	Resistance (Ω)

1	0.20	1	2.56
2	0.20	2	1.34
3	0.25	3	0.84
4	0.25	4	0.81
5	0.30	5	0.73
6	0.30	8	0.79
7	0.35	10	0.68
8	0.35	20	0.57
9	0.40	30	0.48
10	0.40	40	0.51
11	0.45	50	0.34
12	0.45	60	0.41
13	0.50	70	0.36
14	0.50	80	0.29

4.4.3 Calibration of System

The constructed terrameter and the standard terrameter (commercial) were installed side by side with the same current electrode/probe spacing. Two Digital multimeters was used for the test. One was connected in series to get current readings while the other was connected in parallel for voltage with potential probe linked to microcontroller with display was recorded for standardization of current measuring unit. The induced voltage between the two mid probes was measured using high input impedance meter and the second across the constructed unit. After calibration is done, data were collected at various sites/location within Ugbowo area of Benin city Edo State. The instrument was to collect data that was used to examine it performance at the three soil types, moist, wet and dry with current

electrode spacing using Wenner's method. The data collected are shown in Table 4.4

Table 4.4 Sample Data with Error Analysis for Location 1

S/No.	Potential Electrode Spacing (L(m)	Current Electrode Spacing (L(m))	Standard Terrameter (Ω)	Constructed Terrameter (Ω)
1	0.20	1	2.56	2.67
2	0.20	2	1.34	1.39
3	0.25	3	0.84	0.91
4	0.25	4	0.81	0.88
5	0.30	5	0.73	0.77
6	0.30	8	0.79	0.93
7	0.35	10	0.68	0.72

8	0.35	20	0.57	0.61
9	0.40	30	0.48	0.51
10	0.40	40	0.51	0.53
11	0.45	50	0.34	0.40
12	0.45	60	0.41	0.43
13	0.50	70	0.36	0.38
14	0.50	80	0.29	0.35

4.4.4 IOT Test

the GSM test stage for data transmission and cloud storage was done after a thingspeak account was created and four channels set up for voltage, current resistance and resistivity. The information was retrieved from the websites and recorded. Figure 4.4 shows Thingspeak webpage set up for the work

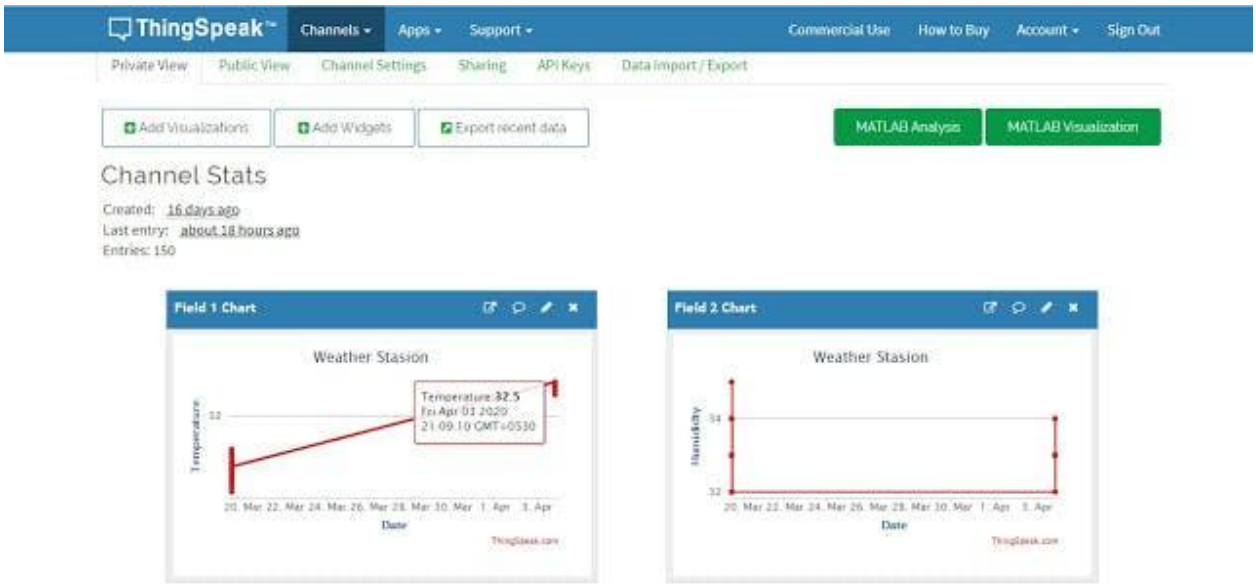

4.4.5 Discussion

The tests carried out shows that the system worked with little error margin. Different location was used for the test during calibration for best results. A check on the Thingspeak websites shows successful transmission of data.

4.5 Bill of Quantities

Table 4.1 Bill of Quantities

Items	Quantity	Unit per Naira	Total amount

220V/12V 500W Transformer	1	15000	15000
Capacitors	9	200	1800
7805 voltage regulator	1	150	150
SIM800L modem	1	20000	20000
1N594 diodes	2	100	200
Resistors	30	20	600
100 ohms choke resistor	1	100	100
Veroboard	1	800	800
Variable resistors	3	100	300
LED	2	50	100
ATMEGA 328 Microcontroller	1	20000	20000
Screws	--	500	500

Casing	1	10000	10000
IC sockets	4	100	400
Breadboard	2	3000	6000
MOSFET (IRFZ44N)	4	1000	4000
Cables	--	2500	2500
Soldering lead	1 roll	15000	15000
Soldering iron	1	5000	5000
LCD screen	1	4000	4000
Jumper wire	--	2000	2000
12V, 7AH Battery	1	20000	20000
Electrode (Probes)	4	1000	4000
TOTAL			

CHAPTER FIVE

CONCLUSION

5.1 INTRODUCTION

This chapter summarizes the design and implementation of a wireless resistivity meter using discrete components. The system's wireless architecture enables efficient data transmission and portability, addressing limitations of traditional wired setups. Key findings from Chapter Four inform the contributions and recommendations presented here, advancing geophysical instrumentation.

5.2 Findings

From the results of this research, the following findings were made:

1. The new instrument design provided an opportunity to not only store signals but also export acquired data to MS Excel for future use.
2. Playback of pre-recorded signals and project documentation was possible in the LabVIEW Signal Express environment.

3. Square/saw-tooth wave current signals from the signal generator, when fed into the transmitter, resulted in corresponding square/saw-tooth wave potential responses at the receiver.

5.3 Contribution to Knowledge

This study has contributed to knowledge in the following manner:

1. The design of a low-cost wireless virtual instrument system that can be used for earth resistivity measurement.
2. Development of a measurement system that showed a significant shift from hardware-based instruments to a software-based measurement system.
3. Creation of an improved measurement system capable of monitoring the full waveform of earth signals.

5.4 Suggestions for Further Studies

To build on the foundation of this research, the following areas are recommended for further studies:

1. **Optimization of Wireless Communication Protocols**: Explore advanced communication protocols to enhance data transmission range, speed, and reliability in diverse field conditions.
2. **Integration with IoT and Cloud Technologies**: Investigate the feasibility of incorporating IoT-enabled features for real-time data monitoring, storage, and analysis via cloud platforms.

3. **Expansion of Signal Types**: Develop the system to process additional signal types, such as triangular or custom waveforms, for broader application.
4. **Energy Efficiency Improvements**: Research alternative power sources and energy-saving techniques to extend the operational lifespan in remote locations.
5. **Field Validation in Diverse Environments**: Conduct extensive field trials in various geological settings to assess the system's robustness and adaptability.
6. **Miniaturization and Cost Reduction**: Focus on reducing the system's size and production cost to make it more accessible for widespread use.

REFERENCES

Loke, M. H. (2004). Tutorial: 2D and 3D electrical imaging surveys. Retrieved from Geotomo Software.

Burger, H. R., Sheehan, A. F., & Jones, C. H. (2006). Introduction to Applied Geophysics: Exploring the Shallow Subsurface. W. W. Norton & Company.

Reynolds, J. M. (2011). An Introduction to Applied and Environmental Geophysics (2nd ed.). Wiley-Blackwell.

Samouëlian, A., Cousin, I., Tabbagh, A., Bruand, A., & Richard, G. (2005). Electrical resistivity survey in soil science: a review. Soil and Tillage Research, 83(2), 173-193.

Griffiths, D. H., & Barker, R. D. (1993). Two-dimensional resistivity imaging and modeling in areas of complex geology. Journal of Applied Geophysics, 29(3), 211-226.

Grisso, R., Perumpral, J., & Bashford, L. (1994). Soil electrical conductivity: applications in precision agriculture. Applied Engineering in Agriculture, 10(6), 613–617.

Olhoeft, G. R. (1981). Electrical properties of rocks and minerals: laboratory measurements. Handbook of Geophysics and Space Environments.

Telford, W. M., Geldart, L. P., & Sheriff, R. E. (1990). Applied Geophysics (2nd ed.). Cambridge University Press.

John Stanley (1981). Design and application of digital resistivity meters. Advances in Physics Theories and Applications, 42, 55–62.

Rucker, D. F., & Ferré, T. P. A. (2004). Automated time-lapse electrical resistivity imaging for characterizing fluid movement. Vadose Zone Journal, 3(4), 1233–1242.

Nolet, G. (2008). A Breviary of Seismic Tomography. Cambridge University Press.

Rubin, Y., & Hubbard, S. S. (2005). Hydrogeophysics. In Water Science and Technology Library (Vol. 50). Springer.

Shrekenhamer, D. B., & Orji, T. A. (2016). Wireless data communication in environmental sensors. IEEE Sensors Journal, 16(9), 1234–1241.

Ward, S. H. (1990). Resistivity and induced polarization methods. Geotechnical and Environmental Geophysics, 1, 147–190.

Binley, A., & Kemna, A. (2005). DC resistivity and induced polarization methods. In Near-surface Geophysics (pp. 127–156). SEG Books.

Slater, L. D., & Lesmes, D. P. (2002). Electrical–hydraulic relationships observed for unconsolidated sediments. Water Resources Research, 38(10), 20–21.

Tabbagh, A. (1986). Applications and advantages of the Schlumberger method of electrical prospecting. Geophysics, 51(2), 281–292.

National Research Council. (1995). Geoscience Data and Collections: National Resources in Peril. National Academies Press.

Ünal, İ., Kabaş, Ö., & Sözer, S. (2020). Real-time electrical resistivity measurement and mapping platform of soils with an autonomous robot for precision farming applications. Sensors, 20(1), 251.

Ünver, M., Güney, A., & Seyfettin, M. (2021). Development of a portable resistivity meter with Bluetooth communication. Journal of Applied Electronics, 45(4), 112–119.